 ISSN: 1857-7881 (Print) e - ISSN 1857-7431

ESJ Natural/Life/Medical Sciences

Akwasi Acheampong Aning,
Geophysics Section, Department of Physics, Kwame Nkrumah University of Science and Technology, Kumasi, Ghana

Van-Dycke Sarpong Asare,
Geophysics Section, Department of Physics, Kwame Nkrumah University of Science and Technology, Kumasi, Ghana

Reginald Mensah Noye,
Geophysics Section, Department of Physics, Kwame Nkrumah University of Science and Technology, Kumasi, Ghana

Submitted: 17 October 2020
Accepted: 23 November 2020
Published: 31 December 2020

Corresponding author:
Akwasi Acheampong Aning

DOI: 10.19044/esj.2020.v16n36p361

Copyright 2020 Akwasi Acheampong A , Distributed under Creative Commons BY-NC-ND 4.0 OPEN ACCES

Cite as:
Akwasi Acheampong A, Van-Dycke Sarpong A, Reginald Mensah N. (2020). Electrical Resistivity And Induced Polarization Imaging For Refuse Dump Site. *European Scientific Journal, ESJ, 16 (36)*, 1. https://doi.org/10.19044/esj.2020.v16n36p361

Electrical Resistivity And Induced Polarization Imaging For Refuse Dump Site

Abstract
Contamination from landfills as a result of leaching from organic and inorganic waste poses a threat to the environment because, subsoil and groundwater are affected. The contamination is more serious in developing countries where waste management is inefficient. The aim of this study was to determine the extent of pollution at this site. Three profiles were surveyed: two in North-South direction and the third in Northeast-Southwest. 2D electrical resistivity and Time Domain Induced Polarization (TDIP) data sets have been acquired along the three profiles in Boadi Community. Electrical resistivity and induced polarization together with excavations were successful in mapping the extent of the leachate plume. The study demarcated clearly three main zones: the first, second and third zones indicated chargeabilities > 12.8 msec near the surface, > 6.4 msec and > 12.8 msec at the base respectively. Similarly, resistivities < 12 Ωm, 12 to 24 Ωm and >192 Ωm for the first, second and third zones respectively were delineated. The relatively lower electrical resistivity areas were thought to be due to the presence of the leachate plume and the comparatively higher chargeability zones were interpreted as duricrust. The relatively lower chargeability represents absence of polarizable materials. The study also delineated the weathered basement granodiorites showing relatively higher resistivities. These TDIP and ERT results show that the methods have been successful in mapping the landfill leachate plume. The results from the resistivity and chargeability compare very well with the excavations.

Subject: Science And Technology

 ISSN: 1857-7881 (Print) e - ISSN 1857-7431

Keywords: Electrical Resistivity, Induced Polarization, Refuse Dump, Mapping, Leachate

Introduction

The geoenvironment is an integral part of human existence which calls for the need to obtain detailed information about it. This information will prove useful for town and country planning, infrastructural development, remediation and the exploration of the natural resources such as water, minerals and oil and gas. There is also an increasing demand for the reuse of abandoned dump sites, cemeteries, mines and even industries indulged in hazardous operations because of the inordinate desire to develop in order to cater for current and future generations.

Uncertain about what underlies the earth's surface, this information is best sought initially through a non-invasive and non-destructive means and the geo-electrical techniques stand out as one of the most suitable methods. The resistivity method has become very popular in electrical exploration because of its ability to produce subsurface images efficiently and effectively owing to available automated data-acquisition systems and efficient user-friendly inversion software (Dahlin and Zhou, 2006). It is based on assumptions that various subsurface earth materials like minerals, solid bedrock, sediments, air and water-filled structures have detectable electrical resistivity contrasts relative to the host medium (Panek et al., 2010). The electrical resistivity method has proven to be credible for site characterization for borehole development (Ogungbe et al., 2010), landfill leachate plume mapping (Maurya et al., 2017), leachate pathways for groundwater contamination (Abdullahi and Osazuwa, 2011) and the detection of groundwater pollutants (Uchegbulam and Ayolabi, 2014). Other studies also confirm its ability to map shallow anomalies (Kumar, 2012; Nero et al., 2016) and also of geological units (faults, fractures and quartzite veins) related to the formation of groundwater systems (Mendoza and Dahlin, 2008).

Engineering, environmental and shallow surface investigations have also emerged as some of the useful applications of the geophysical method (van Schoor, 2002; Aning et al., 2014; Andrews et al., 2013; Ugwu and Ezema, 2013; Obasi et al., 2015; Binley et al., 2015; Panek et al., 2010). The electrical resistivity method has been used prior to constructional projects in mining and abandoned mining areas (Martinez-Pagan et al., 2013; Martinez-Lopez et al., 2013); limestone or dolomite dominant zones which are susceptible to cavity formation due to natural processes (van Schoor, 2002; Metwaly and AlFouzan, 2013) to study the subsurface before the projects were embarked on. In time domain induced polarization (TDIP) surveys, the measured quantity is the chargeability and it is the ratio of the secondary

 ISSN: 1857-7881 (Print) e - ISSN 1857-7431

potential to the primary potential of the transmitted current. The ability of the subsurface to be polarized when electric field is applied is a measure of the induced polarization effect. IP has been used to differentiate between fine-grained and other cover materials in landfill site (Leroux et al., 2007), saltwater intrusion into fresh aquifer (Ranieri et al., 1996), mapping of potential conduit for leachate contamination of the groundwater system (Wemegah et al., 2017), delineating aquifer in sedimentary terrain (Aizebeokhai et al., 2016).

This study also relies on the TDIP and ERT to investigate a refuse dump site to assess the level of pollution and its suitability for future constructional purposes after carefully studying the geology and soils of the place. These methods were chosen as a result of their ability to map waste deposits due to their sensitivity to electrical conductivity and resistivity

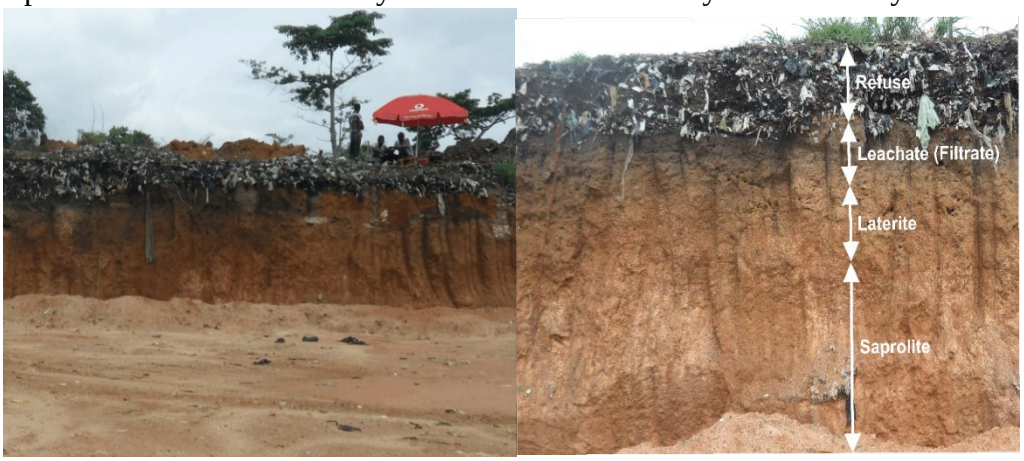

Figure 1. Field photograph with stratigraphy of the study site

2. Geological Setting

The study area (Fig. 1) is located in Boadi, an old town in the eastern part of the Kumasi Metropolis. The area is dominated by the middle Precambrian rocks and forms part of Eburnean Plutonic Suite. These were formed approximately within the upper and lower ages of 2.172 and 2.116 million years ago. The Precambrian rocks and the Eburnean plutonic suite are also composed mainly of biotic (+/-hornblende), granite and minor granodiorite and K-feldspar porphyritic.

 ISSN: 1857-7881 (Print) e - ISSN 1857-7431

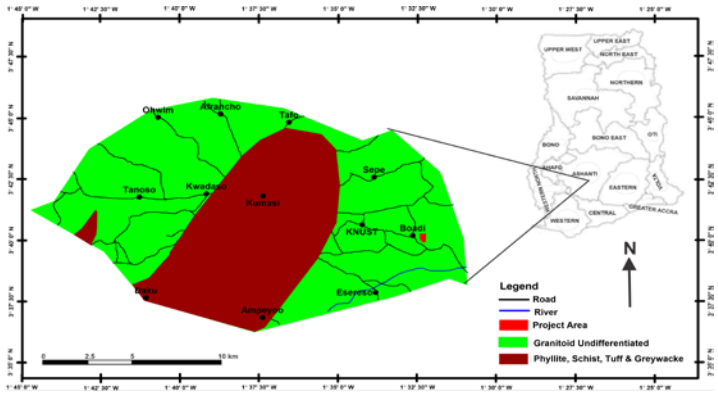

Figure 2. Geological map of the Kumasi Metropolis showing the study area in red (Ghana Geological Survey , 2009)

There are Birimian sequences in the area characterized by a transition in the sedimentary facies from the central part of the basin to the margins. Sediments deposited in the central part consist of a thick sequence of dark grey to black argillites that are interbedded with subordinate siliciclastic meta-sediments. The argillites grade laterally or horizontally away from the centre of the basin into a thick sequence of interbedded argillite/volcaniclastic units and to volcaniclastics interbedded with subordinate argillites, tuffs and volcanics. A narrow belt (up to 3 km wide) underlain by interbedded volcaniclastic and coarse arenaceous sediments such as greywackes, arkose, conglomerates, quartzite etc. also occur (Moon, 1962). These clastic and volcaniclastic units feature high radiometric potassium (K) levels and appear to be somewhat distinctive from most of the typical interbedded volcaniclastic and marine sedimentary units as well as the Tarkwaian clastic sediments (Griffis, 1998). According to Kesse (1969; 1972), the Kumasi granitoid complex dominates much of the basin area and contains large roof pendants of metasedimentary schists. This is a basin-type granitoid massive intrusive complex and ranges in composition from intermediate (granodiorite/tonalite) to more felsic (granite) phases. The construction industry in the metropolis has come to stay because of the existence of the Precambrian rocks. Specifically the study area is covered mainly by the granitoid undifferentiated geology (Fig. 2) and ochrosol soil (Obeng, 2000).

2. Methodology

The survey was performed using the multi-electrode ABEM Lund Imaging System (Dahlin, 1996) with the Wenner array. Three profiles of 60 m each were surveyed with electrode separation of 1.5

m. The 2D apparent resistivity and chargeability (time-domain IP effect) were measured concurrently in all the traverses. The chargeability (M) of the IP effect was determined by integrating the area under the IP decay curve and according to the relation

$$M = \frac{1}{V_0}\int_{t_1}^{t_2} V(t)dt \qquad 1$$

where V_0 is the observed voltage with the applied current, V(t) is the decaying voltage, t_1 and t_2
are the start and stop times respectively. Similarly, the apparent resistivity (ρ_a) was calculated from the equation

$$\rho_a = 2\pi a\left({}^{\Delta V}/_{I}\right) \qquad 2$$

where ΔV is the potential difference, I the applied current and a is electrode separation.

The data obtained from the field are apparent resistivity and chargeability values and must be converted to true resistivity and chargeability values, the variations we are looking for. This transformation from apparent resistivity and chargeability to true resistivity and chargeability is made possible with Res2DINV software. The data were imported into the Res2DInv for processing. The outliers due to poor electrode contact were removed. The algorithm proposed by Loke and Barker (1996) and based on regularized least-squared optimization method (deGroot Hedlin and Constable, 1990; Loke et al., 2003; Sasaki, 1989) for the automatic 2D inversion of apparent resistivity and chargeability data was used. The L_1–norm (the robust) inversion technique was used in modelling the data. Model discretization followed by model refinement with the option of half electrode spacing was applied. The half electrode spacing option step produces better results by narrowing the model cells if there are large resistivity variations near the ground surface. For uniformity in the interpretation of the different true resistivity and chargeability sections along various profiles, a common colour code was adopted for presentation of the results.

Fig. 1 shows fresh excavated section of the Boadi refuse dump site that was leased out to a developer. The first two profiles run parallel to the face of the excavated section and the third oriented approximately 45^0 to it.

3. Results and Discussions

The exposure (Fig.1) showing a four-section vertical zonation allowed detailed analysis of subsurface features of the site. The first or top layer is the refuse with an average thickness of about one metre, is made up of organic

 ISSN: 1857-7881 (Print) e - ISSN 1857-7431

and inorganic matter of degradable material and it is dark in colour. The leached (filtrate) and percolated portion formed the second zone that looks blackish (loamy). The reddish-brown lateritic earth material forms the third zone and the fourth layer is the saprolite, which is light brown and is clayey (shaley). The saprolite layer extends down into the granitic bedrock.

Figs. 3 - 5 show the models obtained from the 2D apparent resistivity and chargeability values of the three survey lines from the Boadi waste dump site after six iterations. The rms errors after the sixth iteration are between 1.2 - 2.9% and 2.0 - 3.6% for the resistivity and chargeability models respectively. The iteration was done to convert apparent resistivity/chargeability values to true resistivity/chargeability values.

Fig. 3 shows the resistivity and chargeability models for profile 1 which trends N-S direction. On this profile, the refuse dump extends from the beginning of the profile to about 43 m. The top 1.5 m from the surface has a heterogeneous nature with resistivity ranging from about 12 to over 200 Ωm (Fig. 3a) and chargeability from a value of 3.2 to above 30 msec (Fig. 3b). The unsorted nature of the resistivity reflects the heterogeneity of the garbage which has led to local changes in the amount of seepage as a result of the waste dump (Fig. 1). The zones marked by the broken black lines on Fig. 3a were interpreted as highly leachate concentration points as a result of the very low

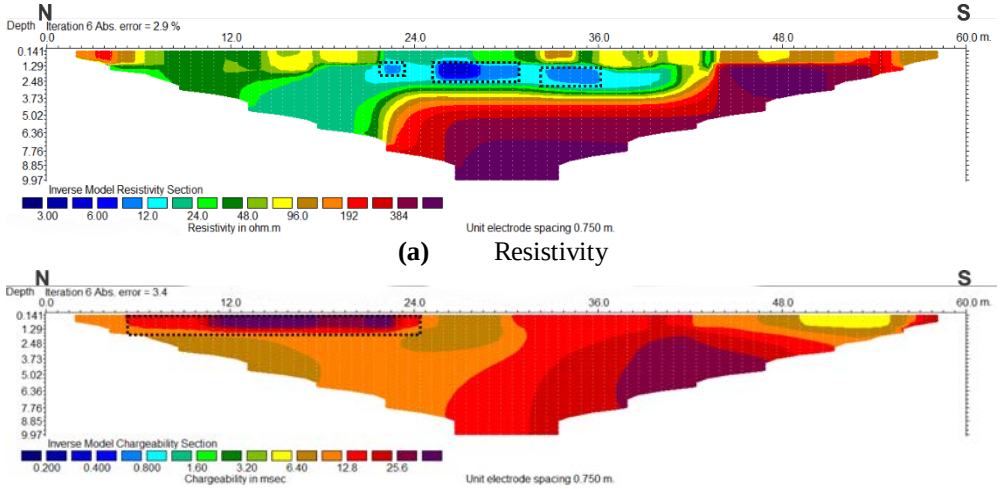

Figure 3. 2D resistivity and chargeability models for profile 1

resistivities (< 12 Ωm) at these areas (Fig. 1). This compares well with works by (Guérin et al., 2004; Zume et al., 2006). The low resistive zone (between 12 and 24 Ωm) is also contaminated areas of varying degrees. The south section of the model below 1.5 m and the base beneath 5 m show no evidence

 ISSN: 1857-7881 (Print) e - ISSN 1857-7431

of contamination by the leachate plume as a result of the high resistivity (> 192 Ωm) and is interpreted to be the weathered bedrock. The relatively higher chargeability region with values greater than 12.8 msec is marked by the black broken lines near the surface (Fig. 3b). The region is about 1.5 m in thickness, and could be due to presence of metallic and polarizable materials that made up the waste. The relatively higher resistive area (> 200 Ωm) at the base which extends towards the south could be the saprolites.

Fig. 4 shows the results for profile 2, which was laid out in N-S direction. The waste dump on this profile spread from 0 - 36 m. The resistivity model section (Fig. 4a) depicts a shallow near surface layer of about 1.3 m thick characterized by high heterogeneity with values ranging from about 20 to 400 Ωm. The differences in the resistivity values could be due to varying concentration of leachate emanating from the waste. The moderately high resistivity (96 to 192 Ωm) area marked by the dotted black line from 7.5 m distance to 18 m and between the depth of 1 and 2.6 m in Fig. 4a could be due to a likely presence of dense duricrusts. The relatively low resistivity signature (48 Ωm) beneath 5 m from 12 to 21 m is interpreted as zone of conductive leachate plume emanating from the waste (Abdullahi et al., 2011; Shemang et al., 2011). The middle portion of resistivity tomography with value > 192 Ωm beneath 1.3 m distance to the end of the profile shows no evidence of leachate plume and this could represent the weathered bedrock. The chargeability model (Fig. 4b) depicts low values (< 6.4 msec) from 0 to 27 m and this may result from lack of highly polarizable materials within the waste. The relatively higher chargeability portion from 27 m to the end of the survey line agrees very well with the resistivity model and is interpreted as the weathered bedrock.

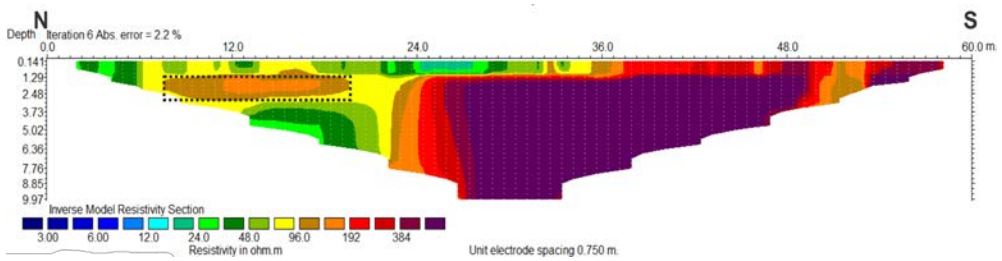

(a) Resistivity

 ISSN: 1857-7881 (Print) e - ISSN 1857-7431

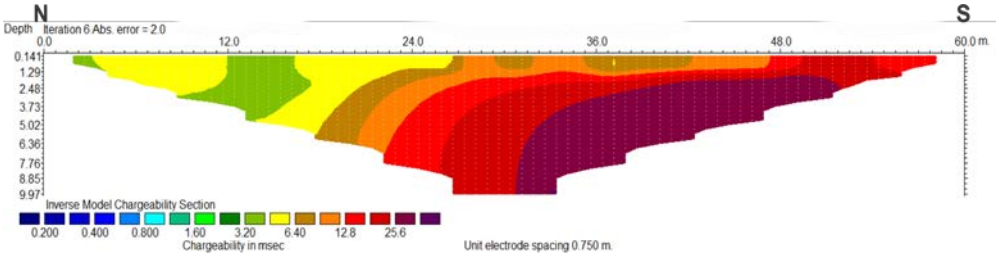

(b) Chargeability

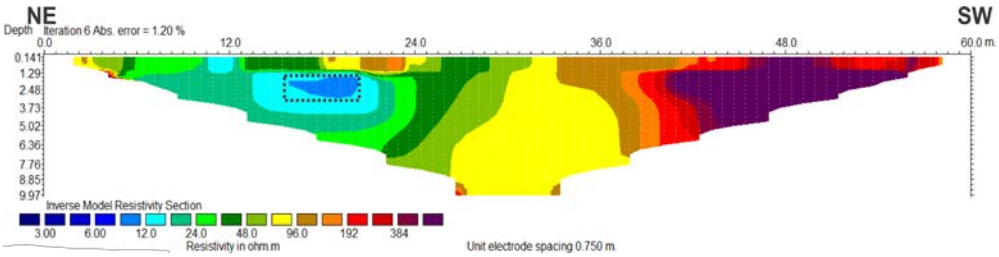

Figure 4. 2D resistivity and chargeability models for profile 2

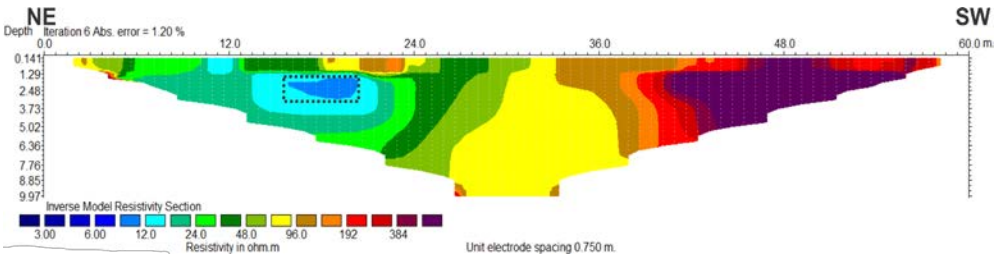

(a) Resistivity

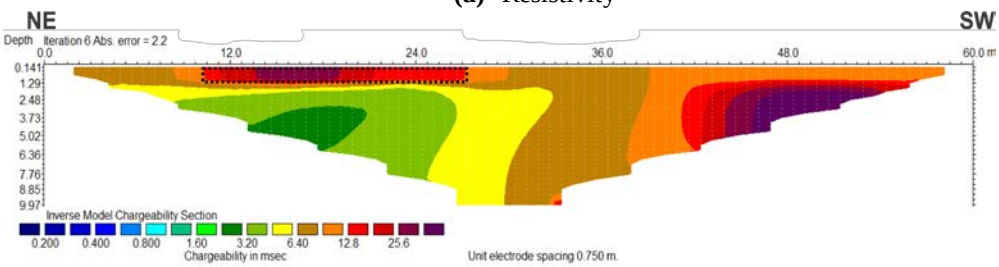

(b) Chargebility

Figure 5. 2D resistivity and chargeability models for profile 3

Fig. 5 shows the 2D inversion results for the resistivity and IP tomography of profile 3 which trends NE-SW. The waste dump on this profile stretches from 0 to 32 m. The heterogeneity of the near surface resistivity model depicts the conglomeration of the waste and different concentration of the leachate plume. The relatively very low resistivity zone (< 12 Ωm) at a depth range of 1.5- 3.0 m and about 4.5 m in length (Fig. 5a)

 ISSN: 1857-7881 (Print) e - ISSN 1857-7431

is interpreted as highly concentrated leachate area. This compares very well with the exposures (Fig. 1). The second half of the resistivity model depicts a relatively high resistive zone (> 96 Ωm) is revealed as weathered bedrock. The relatively higher chargeability layer near the surface (Fig. 5b) beneath and between 10 and 26 m could be as a result of the presence of polarizable materials that may be present in the waste. The relatively low chargeability (< 6.4 msec) stretch beneath 1.3 m may emanate from decrease in ionic mobility as a result of increase concentration of the solution (Maurya et al., 2017). The relatively higher chargeability (> 6.4 msec) section from 33 m corroborate the results of the resistivity model and represents the weathered bedrock.

In all the time domain induced polarization fence diagram (Fig. 6a), three main zones were interpreted. The first zone with relatively higher near surface chargeabilities (> 12.8 msec) is as

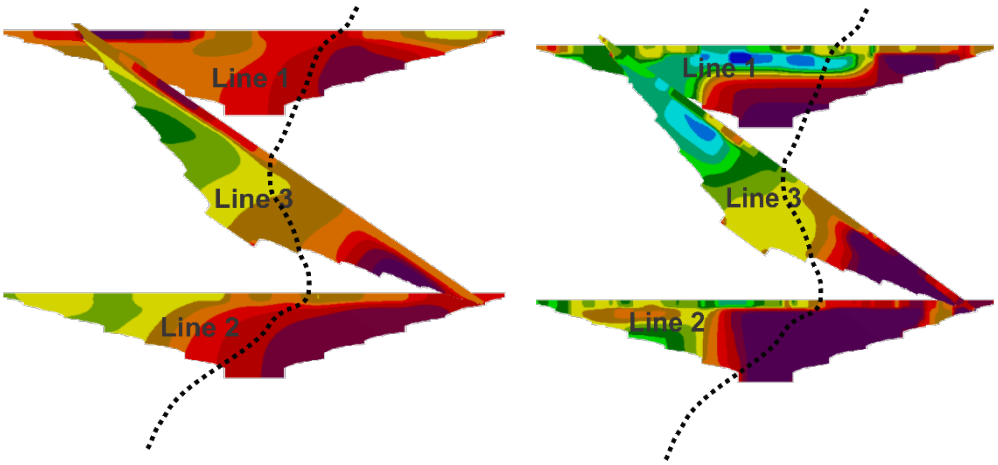

(a) Chargeability **(b)** Resistivity

a result of highly polarizable materials within the waste. The second zone shows a comparatively lower chargeability values (< 6.4 msec) than the first zone. This is possibly due to decrease in concentration of ionic charges. The third zone with chargeability (> 12.8 msec) from the mid portion to the end of the survey line is the saprolite layer. The resistivity fence diagram (Fig. 6b) also depicts three main zones. The first zone with relatively lower resistivity (< 12 Ωm) is the highly concentrated leachate plume zones. The second zone has a varied degree of pollution and has relatively higher resistivity than the first (between 12 and 24 Ωm). The last zone is the weathered bedrock with resistivities > 192 Ωm. The boundary of the landfill is marked by the black dotted line.

Conclusion

The integrated use of non-destructive geophysical techniques; time domain induced polarization and resistivity methods have been successful in characterizing the Boadi waste site. The data from the 2D models were used for the fence diagram. The integration of geology from the excavations, geo-electrical and time domain induced polarization measurements yielded useful information for mapping the site. The results were able to delineate the spatial distribution of the leachate plume due to the fact that in general, for resistivity values < 24 Ωm the area is expected to have high leachate content. Values greater than that were interpreted as weathered bedrock. The results of the study also indicate that higher chargeabilities result from either the weathered bedrock or highly polarizable material and lower values are due to insufficient ionic mobility.

The results show how indiscriminate dumping of refuse pollute the soil and groundwater thereby affecting the environment. For future development plans, the area should be excavated, refill and compacted from the beginning of the profile to the boundaries of the refuse dump up to a depth of about 4 m. This is to make the area more consolidated to support developmental projects in the area.

The overall TDIP and ERT results show that the methods have been successful in mapping the landfill leachate plume and a good correlation exists between the two methods.

References:

1. Abdullahi, N. and Osazuwa, I. (2011). Geophysical imaging of municipal solid waste contaminant pathways. Environmental Earth Sciences, 62(6):1173–1181.
2. Abdullahi, N., Osazuwa, I., and Sule, P. (2011). Application of integrated geophysical tech- niques in the investigation of groundwater contamination: A case study of municipal solid waste leachate. Ozean Journal of applied sciences, 4(1):7–25.
3. Aizebeokhai, A. P., Oyeyemi, K. D., and Joel, E. S. (2016). Groundwater potential assessment in a sedimentary terrain, Southwestern Nigeria. Arabian Journal of Geosciences, 9(7):496.
4. Andrews, N. D., Aning, A. A., Danuor, S. K., and Noye, R. M. (2013). Geophysical investigations at the proposed site of the KNUST Teaching Hospital Building using 2D and 3D resistivity imaging techniques. International Research Journal of Geology and Mining (IRJGM), 3(3):113–123.

5. Aning, A. A., Sackey, N., Jakalia, I. S., Sedoawu, O., Tetteh, E. H., Hinson, G., Akorlie, R. K., Appiah, D., and Quaye, E. (2014). Electrical Resistivity as a Geophysical Mapping Tool; A Case Study of The New Art Department, KNUST-Ghana. International Journal of Scientific and Research Publications, 4: ISSN 2250–3153.
6. Binley, A., Hubbard, S. S., Huisman, J. A., Revil, A., Robinson, D. A., Singha, K., and Slater, L. D. (2015). The emergence of hydrogeophysics for improved understanding of subsurface processes over multiple scales. Water Resources Research, pages 3837–3866.
7. Dahlin, T. (1996). 2D resistivity surveying for environmental and engineering applications. First Break, 14:275–284.
8. Dahlin, T. and Zhou, B. (2006). Gradient array measurements for multi-channel 2D resistivity imaging. Near Surface Geophysics, pages 113–123.
9. deGroot Hedlin, C. and Constable, S. (1990). Occam's inversion to generate smooth two-dimensional models from magnetotelluric data. Geophysics, 55:1613–1624.
10. Ghana Geological Survey (2009). Geological map of Kumasi Metropolis.
11. Griffis, J. R. (1998). Explanatory notes - geological interpretation of geophysical data from South Western Ghana. Mineral Commission, Ghana, Accra., page 51.
12. Guérin, R., Munoz, M. L., Aran, C., Laperrelle, C., Hidra, M., Drouart, E., and Grellier, S. (2004). Leachate recirculation: moisture content assessment by means of a geophysical technique. Waste Management, 24(8):785–794.
13. Kesse, O. G. (1969). The geology of sheet 128, Kumasi, NE. Ghana Geol. Surv. Bull, 39.
14. Kesse, O. G. (1972). The geology of sheet 165, Sekodumasi SW. Ghana Geol. Surv. Bull., 41.
15. Kumar, D. (2012). Efficacy of Electrical Resistivity Tomography Technique in Mapping Shallow Subsurface Anomaly. Journal Geological Society of India, 80:304–307.
16. Leroux, V., Dahlin, T., and Svensson, M. (2007). Dense resistivity and induced polarization profiling for a landfill restoration project at Härlöv, Southern Sweden. Waste Management & Research, 25(1):49–60. PMID: 17346007.
17. Loke, M. H., Acworth, I., and Dahlin, T. (2003). A comparison of smooth and blocky inversion methods in 2-D electrical imaging

surveys. Exploration Geophysics, 34:82–187.
18. Loke, M. H. and Barker, R. D. (1996). Rapid least-squares inversion of apparent resistivity pseudosections by a quasi-Newton method. Geophysical Prospecting, 44:131–152.
19. Martinez-Lopez, J., Rey, J., Duenas, J., Hidalgo, C., and Benavente, J. (2013). Electrical tomography applied to the detection of subsurface cavities. Journal of Cave and Karst Studies, 75(1):28–37.
20. Martinez-Pagan, P., Gomez-Ortiz, D., Martin-Crespo, T., Manteca, J., and Rosique, M. (2013). The electrical resistivity tomography method in the detection of shallow mining cavities. A case study on the Victoria Cave, Cartagena (SE Spain). Engineering Geology, 156:1–10.
21. Maurya, P. K., Rønde, V., Fiandaca, G., Balbarini, N., Auken, E., Bjerg, P. L., and Christiansen,V. (2017). Detailed landfill leachate plume mapping using 2D and 3D electrical resistivity tomography-with correlation to ionic strength measured in screens. Journal of Applied Geo- physics, 138:1–8.
22. Mendoza, J. and Dahlin, T. (2008). Resistivity imaging in steep and weathered terrains. Near Surface Geophysics, pages 105–112.
23. Metwaly, M. and AlFouzan, F. (2013). Application of 2-D geoelectrical resistivity tomography for subsurface cavity detection in the eastern part of Saudi Arabia. Geoscience Frontiers, 4:469–476.
24. Moon, A. P. (1962). The geology of sheet 165, Sekodumasi nw. Ghana Geol. Survey. Bull.
25. Nero, C., Aning, A. A., Danuor, S. K., and Noye, R. M. (2016). Delineation of graves using electrical resistivity tomography. Journal of Applied Geophysics, 126:138–147.
26. Obasi, I. A., Onwe, I. M., and Igwe, E. O. (2015). Geoelectrical subsurface characterization for foundation purposes in the College of Agricultural Sciences (CAS) campus, Ebonyi State University, Abakaliki, Southeastern Nigeria. Journal of Environment and Earth Science, 5(18):42–52.
27. Obeng, H. (2000). Soil classification in Ghana. CEPA 2000. Selected Economic Issues, 3.
28. Ogungbe, A. S., Olowofela, J. A., Da-Silva, O. J., Alabi, A. A., and Onori, E. O. (2010). Subsur-face Characterization using Electrical Resistivity (Dipole-Dipole) method at Lagos State University (LASU) Foundation school, Badagry. Advances in Applied Science

Research, 1(1):174–181.
29. Panek, T., Margielewski, W., Taborik, P., Urban, J., Hradecky, J., and Szura, C. (2010). Gravitationally induced caves and other discontinuities detected by 2D electrical resistivity tomography: Case studies from the Polish Flysch Carpathians. Geomorphology., 123:165–180.
30. Ranieri, G., Ferrero, L., and Godio, A. (1996). A geophysical study of a coastal plane in Sardinia.Annals of Geophysics, 39(1).
31. Sasaki, Y. (1989). Two-dimensional joint inversion of magnetotelluric and dipole-dipole resistivity data. Geophysics, 54(2):254–262.
32. Shemang, E., Mickus, K., and Same, M. (2011). Geophysical characterization of the abandoned Gaborone landfill, Botswana: implications for abandoned landfills in arid environments. International Journal of Environmental Protection, 1(1):1–12.
33. Uchegbulam, O. and Ayolabi, E. A. (2014). Application of Electrical Resistivity Imaging in Investigating Ground Water Pollution in Sapele Area, Nigeria. Journal of Water Resource and Protection, 6:1369–1379.
34. Ugwu, G. Z. and Ezema, P. O. (2013). 2D Electrical Resistivity Imaging for the Investigation of the Subsurface Structures at the Proposed Site for Kauridan Estate at Ibagwa–Nike, Southeastern Nigeria. International Journal of Scientific Research in Knowledge (IJSRK), 1(12):528–535.
35. van Schoor, M. (2002). Detection of sinkholes using 2D electrical resistivity imaging. Journal of Applied Geophysics, 50:393–399.
36. Wemegah, D. D., Fiandaca, G., Auken, E., Menyeh, A., and Danuor, S. K. (2017). Spectral time- domain induced polarisation and magnetic surveying–an efficient tool for characterisation of solid waste deposits in developing countries. Near Surface Geophysics, 15(1):75–84.
37. Zume, J. T., Tarhule, A., and Christenson, S. (2006). Subsurface imaging of an abandoned solid waste landfill site in Norman, Oklahoma. Groundwater Monitoring & Remediation, 26(2):62–69.